J. Phys. D: Appl. Phys. 48 (2015) 265203 (10pp) doi:10.1088/0022-3727/48/26/265203

Control of carbon content in amorphous GeTe films deposited by plasma enhanced chemical vapor deposition (PE-MOCVD) for phase-change random access memory applications

M Aoukar[1,2,3], P D Szkutnik[2], D Jourde[1,3], B Pelissier[2], P Michallon[1,3], P Noé[1,3] and C Vallée[1,2]

[1] University of Grenoble Alpes, LTM, F-38000 Grenoble, France
[2] CNRS, LTM, CEA—LETI, F-38000 Grenoble, France
[3] CEA—LETI, Minatec Campus, F-38000 Grenoble, France

E-mail: christophe.vallee@cea.fr

Received 26 January 2015, revised 22 April 2015
Accepted for publication 29 April 2015
Published 3 June 2015

Abstract

Amorphous and smooth GeTe thin films are deposited on 200 mm silicon substrates by plasma enhanced—metal organic chemical vapor deposition (PE–MOCVD) using the commercial organometallic precursors TDMAGe and DIPTe as Ge and Te precursors, respectively. X-ray photoelectron spectroscopy (XPS) measurements show a stoichiometric composition of the deposited GeTe films but with high carbon contamination. Using information collected by Optical Emission Spectroscopy (OES) and XPS, the origin of carbon contamination is determined and the dissociation mechanisms of Ge and Te precursors in H_2 + Ar plasma are proposed. As a result, carbon level is properly controlled by varying operating parameters such as plasma radio frequency power, pressure and H_2 rate. Finally, GeTe films with carbon level as low as 5 at. % are obtained.

Keywords: PE-MOCVD, PCRAM, OES, XPS

(Some figures may appear in colour only in the online journal)

Introduction

Among the emerging resistive memory technologies (ReRAM), phase change random access memory (PCRAM) is considered to be one of the most promising candidates for the next generation of nonvolatile memories (NVM). PCRAM are based on the fast and reversible switch between the high resistive amorphous state and the low resistive crystalline state of a phase change material (PCM). The transition from the amorphous to the crystalline phase is obtained by heating the PCM above its crystallization temperature. The reverse operation, which consists to switch back to the amorphous phase, is realized by melting the PCM then quenching the liquid phase fast enough so that it solidifies in the amorphous state.

PCRAM feature many attracting properties such as fast programming speed, very good endurance, excellent data retention and high scalability [1]. All these characteristics make PCRAM the best ReRAM candidate for replacing the currently dominating Flash technology which is based on charge storage, in particular at the smallest CMOS technology nodes (<28 nm) [2].

The phase change materials are generally based on chalcogenide alloys. $Ge_2Sb_2Te_5$ (GST) and GeTe are among the most commonly studied materials for PCRAM applications

 © 2015 IOP Publishing Ltd Printed in the UK

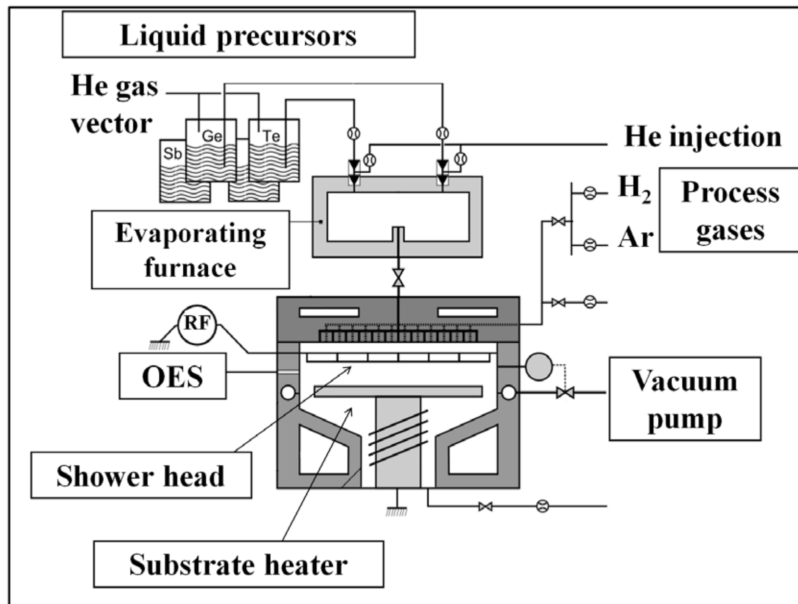

Figure 1. Schematic representation of the AltaCVD200 Advanced Materials™ deposition chamber.

since those GeSbTe-based alloys have been largely used for optical storage (CD-RW and DVD-RW). However, thanks to a higher crystallization temperature compared to GST, GeTe permits a much better data retention in devices and is also a promising candidate for embedded applications [3]. The PCRAM data retention is defined by the capability to keep the amorphous state of the PCM that tends to crystallize with time and temperature.

Nevertheless, high power consumption during the RESET operation is a major limitation for the PCRAM technology, in particular at the lowest CMOS technological nodes for which PCRAMs are expected to replace the current Flash memories. It has been shown that by adopting a confined structure instead of a conventional planar structure, the RESET current required to amorphize the PCM can be significantly reduced [4]. Indeed, a confined-cell structure leads to an improved heating efficiency of the memory cell and thus, to a lower RESET current thanks to both minimizing the PCM active volume and reducing the heat loss [5, 6]. In order to achieve such confined structure device, a highly conformal process is required. Due to its inherent poor step coverage, conventional physical vapor deposition (PVD) process cannot be used for future PCRAM applications. Considering the low deposition rate of atomic layer deposition (ALD), metal organic chemical vapor deposition (MOCVD) seems to be the most suitable technique to achieve the gap filling of PCMs in high aspect ratio structures. Even though MOCVD offers better conformity than PVD, it suffers from organic groups or atoms contamination (mainly C and H) resulting from the precursors dissociation. In the case of PCM, the incorporation of carbon has a beneficial effect on the films properties. Indeed, recent studies [7–9] have shown that doping GeTe or GST with carbon or nitrogen increases their crystallization temperature with an increase of data retention at high temperature. However, high carbon doping drastically reduces the crystallization speed and the programming window of PCRAM cells [9]. Therefore, in order to take advantage of the carbon doping, carbon level should be accurately controlled in the deposited layer.

In this work, we first report the deposition of amorphous, homogeneous, and smooth layers of GeTe, which is crucial for good conformal deposition, by using a plasma enhanced MOCVD process (PE-MOCVD). Then, we study the precursors dissociation mechanisms in the deposition plasma, by means of optical emission spectroscopy (OES) coupled with analysis of films by *quasi in situ* x-ray photoelectron spectroscopy (XPS). This study gives us clues on how to control C contamination in the films. Finally, we show that the carbon concentration level, and consequently the crystallization temperature of GeTe layers are controlled by a proper tuning of the deposition operating parameters.

Experimental setup

GeTe films are grown on 200 mm silicon substrates using a pulsed liquid injection system mounted on a PE-MOCVD reactor supplied by the ALTATECH company (AltaCVD200) [10]. A scheme of the system is shown in figure 1. The injection stage is a patented system [11] in which each injection head is composed of a liquid injector, a mixing chamber and a mixture injector. The liquid precursor is pulsed by the liquid injector into the mixing chamber where it is blended with a carrier gas (helium has been selected to avoid any reaction with the precursor). Finally, this gas/liquid mixture is pushed by the mixture injector in a pulsed regime into a vaporization chamber (or evaporating furnace) where it will be 'flash evaporated'. The injection frequencies and pulses widths allow us to precisely control the amount of precursors supplied in the gas phase. Then, the vapor mixture of precursors and process gases are simultaneously introduced into the process chamber through a polarizable and heated dual channel shower head (T_{shower} = 65 °C). Capacitive radio frequency

plasma (RF frequency of 13.56 MHz) is applied between the shower head and the substrate heater. To avoid condensation of precursor vapors, the chamber's walls are heated at 70 °C. The residual organic compounds and by-products are evacuated by a vacuum pump through a rotating valve that regulates the pressure in the deposition chamber during the process.

The nature of the process gases introduced in the deposition plasma is crucial since it is an important parameter for reducing the carbon level in the deposited films. Generally, oxygen or hydrogen is commonly used to reduce the carbon level. In our case, to avoid any oxidation of the PCM, metal organic precursors will be injected in a H_2 + Ar plasma.

An optical emission spectroscopy (OES) system directly mounted on the deposition vessel is employed as a gas phase diagnostic tool in order to obtain information about the formation and the density of excited-state species during the deposition. OES allows a better understanding of the overall deposition process mechanism. The plasma was monitored by a 'Horiba Endpoint Monitor EV-140 C' with an optical resolution <2.0 nm in the 200–500 nm range and <2.5 nm for 500–700 nm range. The optical emission spectra were recorded in the range 200–800 nm at a frequency of one spectrum each 300 ms.

The films morphology was studied by scanning electron microscopy (SEM). The compositions and chemical bonding of the deposited films were analyzed by *quasi in situ* x-ray Photoelectron Spectroscopy (XPS). The XPS measurements were performed on Thermo Scientific Theta 300 spectrometer with a high resolution monochromatic Al kα x-Ray source (1486 eV) at pass energy of 100 eV and energy step of 0.1 eV. We note that the deposition tool is connected to a specific vacuum carrier developed by Adixen that allows the transfer of the substrate under clean and moisture/oxygen free environment. Such a system avoids the oxidation and limits the carbon contamination of the sample surface allowing thus *quasi in situ* XPS analysis [12]. The relative atomic concentrations of Ge, Te and C were extracted from the Ge 3d, Te 4d and C 1s core level energy regions respectively. Peak contributions were extracted with a combination of Lorentzian and Gaussian functions. The background was subtracted using Shirley function. After correction of the lens transmission factor, each element relative atomic concentration was obtained by dividing calculated peak areas by the corresponding Scofield cross section (Ge 3d: 0.842—Te 4d: 2.140—C 1s: 1.000) [13].

The reflectivity measurements were carried out by monitoring the reflectivity of the PCM samples under Ar atmosphere with a laser probe (0.5 mm diameter) at 670 nm as a function of the temperature (heating rate = 10 °C min^{-1}). The as-deposited films are in amorphous state characterized by a low reflectivity. The crystallization is detected by a significant increase of the sample surface reflectivity. The crystallization temperature is defined as the maximum of derivative of the measured reflectivity curve.

Results and discussion

First of all, a GeTe layer is grown by dissociating the organometallic precursors TDMA-Ge [$Ge(NMe_2)_4$] and DIP-Te [$Te(i\text{-}Pr)_2$] in a H_2 + Ar RF plasma. The plasma is operated at a pressure of 5 Torr, a RF power of 200 W, with a total gas flow rate of 1000 sccm H_2 + Ar (1:1). In this paper, these plasma parameters are considered as our reference deposition conditions. Since in PE-CVD process, the plasma plays a major role in the precursors dissociation, the substrate temperature is reduced below the GeTe crystallization temperature [14]. Consequently, GeTe films are awaited to be deposited in their amorphous state and thus better deposition conformity is expected. Substrate temperature is fixed at 160 °C which is approximately 20 °C lower than the generally reported crystallization temperature of GeTe thin films [15].

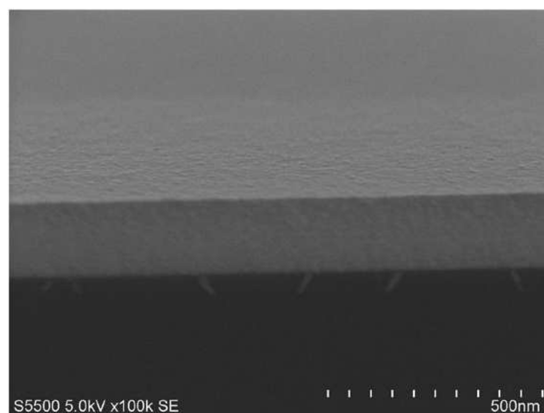

Figure 2. SEM cross section view of a GeTe film deposited in the reference conditions [T = 160 °C; P= 5 Torr; RF=200 W; 1000 sccm H_2 + Ar (1:1)].

The SEM image of a GeTe film deposited in the reference conditions, shown in figure 2, reveals a homogeneous and smooth layer with a mean thickness of 200 nm corresponding to a deposition rate of 10 nm min^{-1} which is compatible with industrial requests.

XPS analysis is then conducted for purposes of characterizing the chemical composition and the atomic bonding state of the as-deposited GeTe film. In the XPS wide spectrum (figure 3(a)), the presence of Ge, Te and C is evidenced. We note that no trace of N is detected by XPS although it is present in the Ge precursor's molecule. We also note the absence of O peak, which proves that the oxidation of the film did not take place during the transfer. The atomic concentration of each element is calculated as described in the experimental section. The resulting Ge/Te ratio is of 1.14 which is close to the target stoichiometric composition. However, a C contamination level as high as 16 at. % is found in such GeTe film. Figure 3(b) shows the XPS narrow-scan spectrum of the C1s core level. The C1s peak is well fitted using two contributions: a first one at 284.3 eV attributed to C–H bonds and a second one at lower energy at 283.4 eV corresponding to C–Ge(Te) bonds. Taking into account the electro negativities of Ge, Te and C (respectively 2.01, 2.1 and 2.55 on Pauling scale), C bonded with Ge and Te is expected to imply a shift of the C1s peak toward lower energies which is experimentally observed here. The presence of C–Te and C–H bonds in the material can be easily explained by the direct incorporation of Te–CH_x radicals coming from the Te precursor dissociation in the plasma.

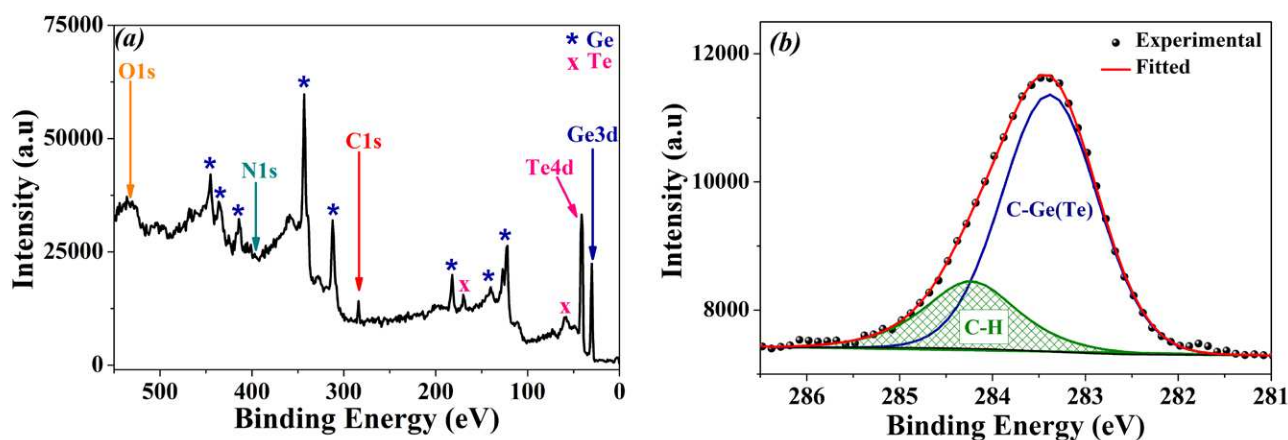

Figure 3. XPS spectra of as-deposited GeTe thin film: (a) Large survey that confirms the presence of Ge, Te and C elements and the absence of N and O (b) Zoom on C1s energy range with dots as the experimental data and continuous line as the result of the fit using two main C environment contributions: C–H (hatched area) and C–GeTe (blank area).

The presence of Ge–C bonds is more complex to explain since there are no such bonds in the Ge precursor. There are only Ge–NCH_x groups. Generally, in PECVD processes, the chemical bonds in the deposited film are similar to bonds in the precursor due to the direct incorporation of radicals coming from the precursor dissociation [16]. The presence of Ge–C bonds suggests that second order reactions occur during the deposition to create the Ge–C bonds. This will be discussed later. This is also supported by the fact that no Ge–N bonds are observed by XPS. We note that C–H bonds can also come from the dissociation of Ge precursor in the plasma.

The presence of hydrogen in the GeTe films is confirmed by elastic recoil detection analysis (ERDA) with a measured atomic percentage of 24%.

In order to check the crystallization temperature of such as-deposited GeTe film, a reflectivity measurement is carried out and is shown in figure 4. An abrupt increase of the reflectivity at T_c = 380 °C is attributed to the amorphous to crystalline transition. This crystallization temperature is notably higher than the one measured for a GeTe carbon free reference sample obtained by PVD (T_c = 180 °C) which corresponds to the value generally reported in literature for pure GeTe [17].

This increase in the crystallization temperature T_c for the PE-MOCVD GeTe film is related to the high carbon content in the deposited films. Moreover, T_c of the PE-MOCVD GeTe film is similar to the one obtained for a PVD GeTe film intentionally doped with at least 15 at.% of C [17]. This is a proof of the effect of carbon incorporation and its inherent doping effect on the crystallization temperature of PCMs, as discussed in the introduction. The challenge now is to be able to control the level of C concentration in the material in order to precisely control the PCM crystallization temperature needed for the devices.

As mentioned before, C contamination results from the dissociation of metal organic precursors in the plasma. The first objective is to determine the contribution of each of the precursors (Ge and Te) in the total C level. For this end, Ge and Te were deposited separately in the reference deposition conditions mentioned previously. Using the information collected by OES, we investigate the dissociation mechanisms

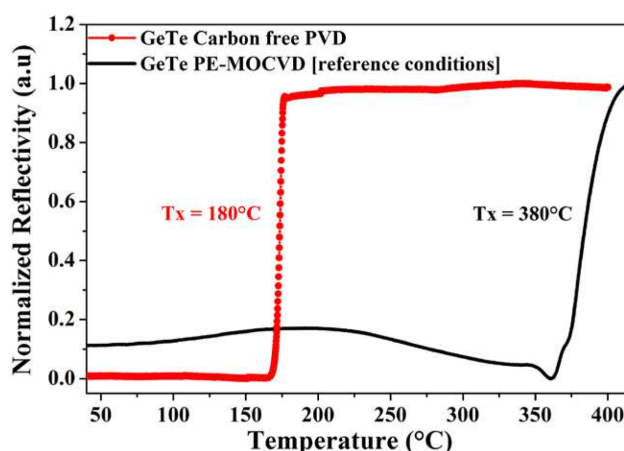

Figure 4. Normalized optical reflectivity curves of a PE-MOCVD GeTe thin film and a reference PVD carbon free GeTe sample as a function of temperature (heating ramp rate 10 °C/min).

that rule the process. This may help optimizing the process and controlling the C level in the deposited films.

Optical emission spectroscopy of deposition plasmas

OES of a pure H_2 + Ar plasma. All experiments are carried out in a H_2 + Ar plasma. Figure 5 shows the optical emission spectrum in the 200–800 nm range of a pure H_2 + Ar plasma which will be considered as the background spectrum of the process. The optical emission spectrum has been divided into two spectral ranges for more clarity. The emission peaks were identified using reference books for atomic lines [18] and molecular structures [19]. The examined emitting species and their spectral characteristics are listed in table 1.

OES of (H_2 + Ar) + [Te(i-Pr)$_2$] plasma. As shown in figure 6(a), the dissociation of the Te MO precursor in the H_2 + Ar plasma leads to the appearance of new emission lines in the 200–450 nm range. These peaks at 225.9, 238.6 and 253 nm can be attributed to Te* emission lines [20]. No emission of CH, CH^+ or C_2 excited species were detected in the spectrum.

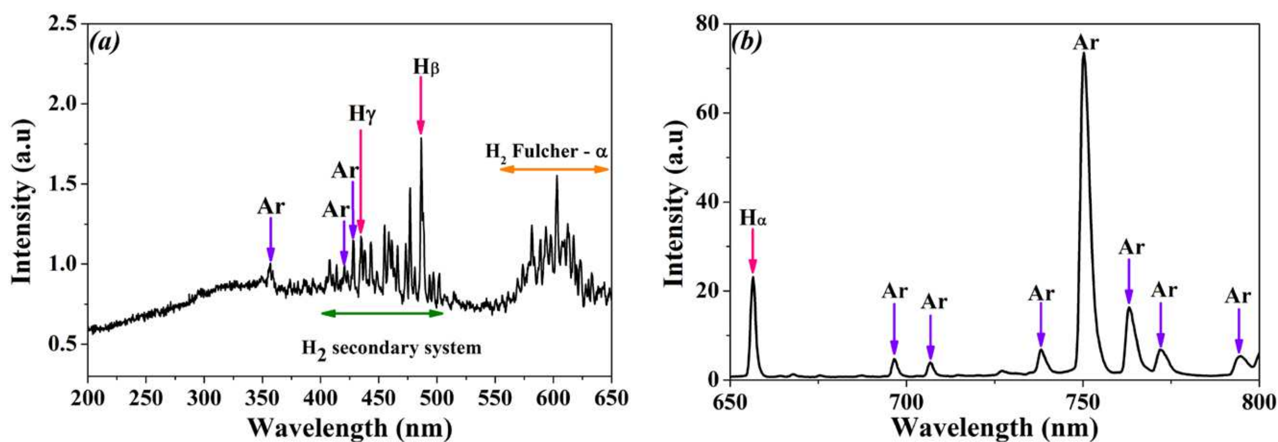

Figure 5. Emission spectra recorded for a H_2 + Ar plasma in the range (a) 200–650 nm (b) 650–800 nm.

Table 1. Emission lines identified in a H_2 + Ar plasma (RF power 200 W—pressure 5 Torr—total gas flow 1000 sccm H_2 + Ar (1:1)).

Species	System name	Wavelength (line) or spectral range (system)
Ar		356.1, 420.0, 427.7, 696.5, 706.7, 738.4, 750.4, 763.5, 772.3, 794.8 nm
H	Balmer lines	H_α 656.3 nm, H_β 486.1 nm, H_γ 434.0 nm
H_2	H_2 secondary system	400–500 nm
	H_2 Fulcher-α	580–650 nm

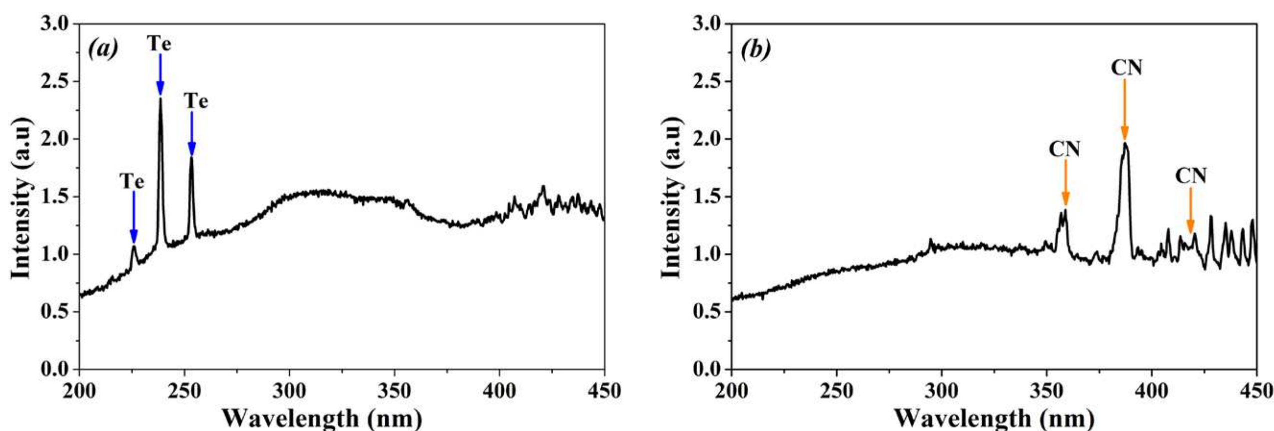

Figure 6. Emission spectra recorded from 200 to 450 nm during the deposition of (a) Te thin films and (b) Ge thin films from their DIP-Te and TDMA-Ge MO precursors in a H_2 + Ar plasma. The non marked bands on the spectra correspond to H_2 + Ar plasma emission lines.

The XPS analysis of Te films reveals a surface composition of 98 at. % of Te and 2 at. % of C. This very low percentage of carbon on the surface of the film is not significant and is most probably due to a residual organic contamination generated by the PECVD process.

Usually, in plasma generated at low pressure using high-density sources such as electron cyclotron resonance (ECR), Inductively coupled plasma (ICP) or helicon, the precursors are dissociated by electron impact thanks to the high electron density. However, since we are using a hydrogen rich plasma operated at high pressure ($P > 1$ Torr), precursors are dissociated by either electron impact or hydrogen radicals. Unfortunately, available data is not sufficient for identifying which mechanism is responsible for the dissociation.

The presence of Te atomic lines in the optical emission spectrum leads to the assumption that both Te–CH bonds in Te precursor are broken to release atomic Te in the gas phase. Consequently, Te is the primary product of the dissociation reaction of Te precursor.

If the dissociation is by electron impact, the reaction is written as follows:

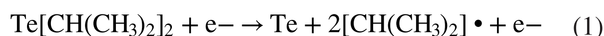

$$Te[CH(CH_3)_2]_2 + e- \rightarrow Te + 2[CH(CH_3)_2] \bullet + e- \quad (1)$$

This dissociation reaction leads to the production of C_xH_y radicals that are known to be highly reactive in the plasma. These reactive species either react in the gas phase or are adsorbed on the surface of the deposited films. The absence of C–H and Te–C bonds in Te films shows that radicals

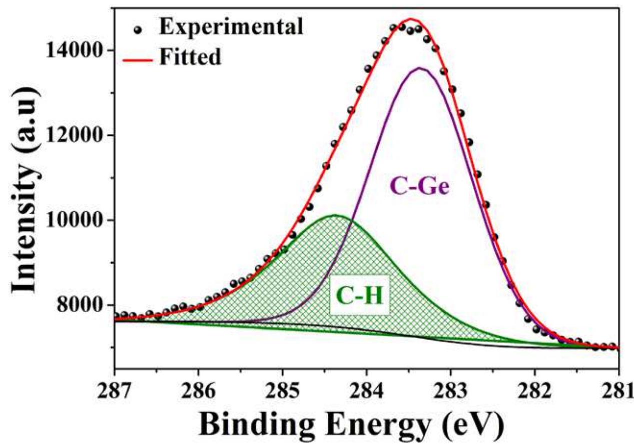

Figure 7. Experimental C1s XPS narrow scan (dots) for Ge films deposited in the reference conditions fitted (continuous line) with 2 contributions C–Ge (blank area) and C–H (hatched area).

recombine with hydrogen radicals and form volatile hydrocarbon which are easily evacuated out of the chamber by the vacuum pump (reaction (2)).

$$[CH(CH_3)_2]\bullet + H\bullet \rightarrow (CH_3)_2CH_{2(g)} \quad (2)$$

If the dissociation is by reaction with hydrogen radicals, the reaction is written as follows:

$$Te[CH(CH_3)_2]_2 + 2H\bullet \rightarrow Te + 2[(CH_3)_2CH_2]_{(g)} \quad (3)$$

As described in reaction (3), the dissociation by hydrogen radicals also leads to the formation of volatile hydrocarbon.

In both dissociation mechanisms, the organic fragment $[CH(CH_3)_2]$ can dissociate to smaller fragments such as CH_x ($x < 4$). These volatile and light fragments tend to recombine with hydrogen radicals and form stable CH_4.

To summarize, when introduced in Ar + H_2 plasma, Te precursor molecules dissociate into atomic Te and organic compounds that are eliminated from the process, resulting in carbon free Te films.

OES of (H_2 + Ar) + [Ge(NMe_2)$_4$] plasma. During the deposition of Ge films with TDMA-Ge MO precursor, large peaks appear around 358, 387 and 420 nm in the 200–450 nm range (figure 6(b)). These large peaks are formed by combining multiple emission bands that correspond to CN violet system [19]. Unfortunately, the low resolution of the optical emission spectrometer does not allow to distinguish these bands. For example, the peak around 387 nm is the result of the combination of CN (0,0), (1,1) and (2,2) bands at 388.3, 387.1 and 386.2 nm respectively [19]. The presence of CN emission lines in the optical emission spectrum is not surprising since C–N bonds are present in the Ge precursor. However, Ge* emission lines expected at 265.1 and 303.9 nm [19, 20] are not visible in the spectrum. Moreover, CH, CH^+, C_2 and NH emission lines are also not observed in the spectrum.

The XPS measurements reveal a C concentration of 30 at. % in Ge films. In figure 7, the C1s XPS narrow scan spectrum shows, as in the above case of GeTe, two contributions that correspond to Ge–C and C–H bonding states. We note that even in the case of Ge films, no trace of nitrogen is detected by XPS.

In our experimental conditions, the presence of carbon cannot be correlated to the presence of CH, CH^+ or C_2 emission lines or not, in the optical emission spectrum. In fact, in the case of Te deposition, the films are carbon free and CH, CH^+ and C_2 emission lines are not detected in the gas phase. However, in the case of Ge deposition, the films contain a high percentage of carbon, even though these emission lines are still not detected in the plasma.

Absence of radicals emission lines in the optical emission spectrum does not imply their absence in the gas phase. It is well known that plasma radicals can exist on non emitting states (ground or even excited levels). However, the absence of Ge emission lines in our experimental plasma conditions is due to the absence of atomic Ge in the plasma. In fact, Ge emission lines are detected by OES in H_2 + Ar plasma (identical to the deposition plasma) when used for cleaning the chamber. This confirms that Ge emits in our experimental conditions and can be detected by OES. Thus, the absence of Ge emission lines during the deposition is indeed due to the fact that atomic Ge is not released in the gas phase when TDMAGe precursor is dissociated in the plasma. Taking into account the above observations and the presence of Ge–C bonds (initially not present in the Ge precursor), we propose the following dissociation mechanism.

First, a carbon–nitrogen rearrangement or transposition reaction takes place in the presence of hydrogen radicals (reaction (4)). The reaction consists in a methyl radical $CH_3\bullet$ migration to the germanium atom with expulsion of the methylamine radical. A similar transposition reaction is proposed by Caubet *et al* during the deposition of TiN using Ti[N(CH_3)$_2$]$_4$ (TDMAT) precursor by PE-ALD [21]. In order to confirm this transposition reaction, we deposit Ge films in pure Ar plasma. XPS measurements (not shown here) on these films reveal a very weak percentage of Ge–C bonds. The carbon is mainly incorporated as C–H, C–C and C–N bonds. This experiment highlights the role of hydrogen radicals in the formation of Ge–C bonds in Ge films.

The methylamine radical is then dissociated either by electron impact or by hydrogen radicals (reaction (5*a*) and (5*b*) respectively), and produce CN and hydrogen. Since no trace of nitrogen was detected by XPS analysis, we assume that CN radical recombine with hydrogen radicals to form the volatile gas HCN (reaction (6)).

The Ge–N(CH_3)$_2$ bonds are also dissociated which results in the formation of several organic fragments. These fragments recombine with hydrogen radicals and form volatile stable hydrocarbons that are pumped out of the process chamber. Reaction (7) shows an example of the dissociation reactions.

As in the case of Te, it is difficult to specify whether dissociation reactions are by electron impact or by hydrogen radicals. Therefore, both hypotheses are maintained.

$$[(CH_3)_2N]_3Ge{-}N(CH_3)(CH_3) + H^{\bullet} \rightarrow [(CH_3)_2N]_3Ge{-}C + CH_3N^{\bullet} \quad (4)$$

$$CH_3N^{\bullet} + e^- \rightarrow CN^{\bullet} + 3H^{\bullet} + e^- \quad (5a)$$

or

$$CH_3N^{\bullet} + H^{\bullet} \rightarrow CN^{\bullet} + 2H_2 \quad (5b)$$

$$CN^{\bullet} + H^{\bullet} \rightarrow HCN_{(g)} \quad (6)$$

$$[(CH_3)_2N]_3Ge{-}C + 3H^{\bullet} \rightarrow H{-}Ge{-}C + 3(CH_3)_2NH_{(g)} \quad (7)$$

When Ge–N bonds are broken, Ge can form bonds with hydrogen or other germanium atoms. The presence of Ge–H is confirmed by Fourier Transform InfraRed (FTIR) spectroscopy (not shown here).

Hydrogen radicals can also play a major role in reducing carbon content in Ge films as described in the following reaction:

$$H{-}Ge{-}C + H^{\bullet} \rightarrow H{-}Ge + CH_{4(g)} \quad (8)$$

Reactions above, highly consistent with what is observed in OES and XPS, describe potential mechanisms in the deposition plasma.

The main conclusion of these experiments is that Ge precursor is clearly the main source of C contamination in our PE-MOCVD GeTe films.

Effect of plasma parameters on C contamination

As demonstrated above, C contamination is mainly due to the dissociation of the Ge precursor. In this section we study the effect of plasma parameters such as RF power, pressure, and gas rate, on the C level in Ge films.

Radio frequency power. The first parameter we investigate is the plasma RF power. The Ge precursor (TDMA-Ge) is injected in a H_2 + Ar (1:1) plasma with a total flow rate of 1000 sccm at a constant pressure of 5 Torr. The RF generator output power varies from 100 to 300 W. Figure 8 shows the normalized intensity of CN and H_α ($I_{CN}/I_{Ar\ 750.4nm}$ and $I_{H\alpha}/I_{Ar\ 750.4nm}$) as a function of the RF power. The intensity of the emission lines of CN and H_α are normalized by the emission intensity of Ar line at 750.4 nm, in order to eliminate the influence of changes in electron energy distribution functions (eedfs). The C at. % in the deposited Ge films, obtained by XPS, is also plotted on the same graph.

By increasing the power, C level and normalized intensities of CN and H_α increase. The increase of normalized intensities is a result of an increase of their densities in the plasma.

The increase of carbon content in Ge films can be associated to two different phenomena.

One possible scenario would be the increase of hydrogen radical density in the plasma due to a more efficient dissociation of H_2 molecules with increasing RF power. In fact, figure 8 highlights a strong correlation between C content in the material and hydrogen radicals density in the plasma. The latter promotes the transposition reaction (4), resulting in an increase of Ge–C bonds.

Another possible scenario would be the increase of carbon content due to a more efficient dissociation of the TDMA-Ge MO precursor which results in a large amount of small organic fragments that cannot be easily eliminated by hydrogen radicals. In that case, the hydrogen rate should be increased in the plasma to reduce all the organic fragments.

Similar results (not shown here) are obtained in the case of GeTe when both precursors are injected in the plasma.

Pressure. In order to probe the effect of the deposition pressure, a similar study to the one previously shown is done by increasing the total pressure in the deposition chamber from 5 to 10 Torr. In figure 9 are plotted the evolution of the C content

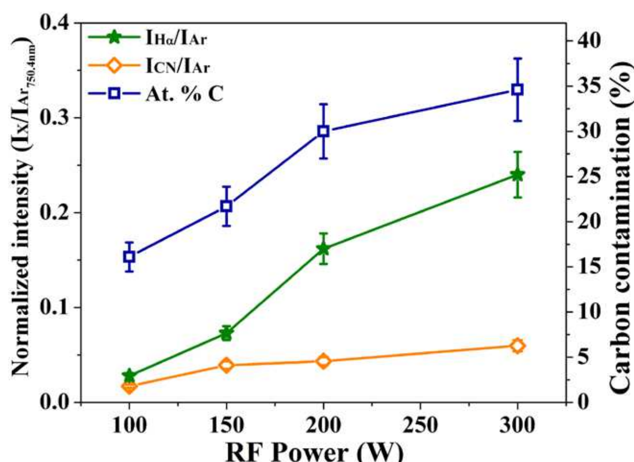

Figure 8. Normalized intensities of CN and Hα plotted with corresponding C content in Ge films as a function of the plasma RF power for a fixed pressure of 5 Torr and a constant H_2/Ar (1:1) total flow rate of 1000 sccm.

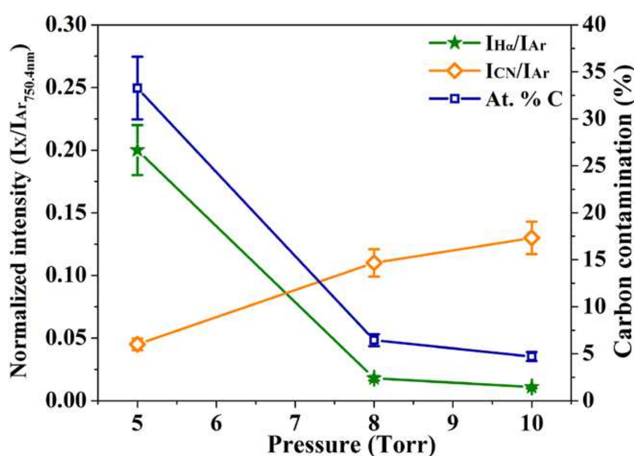

Figure 9. Normalized intensities of CN and Hα and C content as a function of total pressure in the deposition chamber for a fixed plasma RF power of 200 W and a constant H_2/Ar (1:1) total flow rate of 1000 sccm.

in Ge films and normalized intensities of CN and H_α as a function of the deposition pressure for a fixed plasma RF power of 200 W and a constant H_2/Ar (1:1) total flow rate of 1000 sccm.

The percentage of C measured by XPS significantly decreases with the increase of pressure. We notice the persistence of the strong correlation between the evolution of H density and C content in the film.

One possible explanation is the decrease of the dissociation rates of molecules present in the gas phase when pressure increases. As a result, the density of hydrogen radicals and organic fragment decrease in the plasma. The decrease of hydrogen radicals limits the formation of Ge–C bonds through reaction (4). Moreover, the decrease of organic fragment density makes their elimination easier. Thus carbon content is reduced in the deposited films.

Another possible explanation is that the increase in pressure causes a decrease in the mean free path resulting in an increase in gas-phase rates [22]. The collisional interactions promote recombination reactions between organic fragments

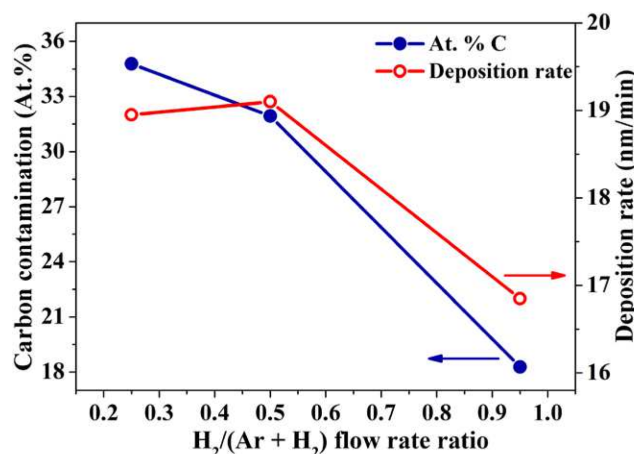

Figure 10. Carbon level and deposition rate as a function of (H_2/(Ar + H_2) flow rate ratio in the deposition plasma.

and hydrogen radicals resulting in a decrease of C level in Ge films.

Gas rate. As shown above, H radicals play a major role in the control of C level in the deposition process with MO Ge precursor. For this reason, we investigate in this section the influence of the H_2 flow rate on the C content.

Ge films are deposited in plasmas with different H_2/(Ar + H_2) flow rate ratios. A total flow rate of 1000 sccm, a total pressure of 5 Torr and a RF power of 200 W are kept constant for all these experiments. As shown in figure 10, the C content in Ge films decreases continuously with the increase of H_2 ratio in the total flow rate.

The density of hydrogen radicals increases with the H_2 flow rate, which allows the elimination of organic fragments by recombination reactions. Thus, the carbon content decreases in the deposited layers.

A complete understanding of mechanisms that occur when the operating parameters are changed is difficult to establish. This is due to the complexity of plasma reactions and the lack of information on the plasma composition and plasma parameters such as electron energy distribution functions (eedfs). In this work, we assume that hydrogen radicals play a major role in the control of carbon content; nevertheless the possibility of molecular hydrogen having a similar role cannot be completely eliminated.

Figure 10 also shows that in hydrogen-rich plasma the deposition rate decreases. This is due to a competitive effect between deposition of GeC_xH_y groups and etching of C_xH_y at the surface, or a chemical etching of Ge by hydrogen radicals. In order to verify the possibility of Ge etching, we proceeded to the following experiments. A silicon substrate on which a Ge film is deposited is introduced into the chamber. In a first experiment an Ar rich plasma is applied to the sample, while in a second test a hydrogen rich plasma is used. As shown in figure 11, the intensity of the Ge emission line is significantly higher for a H_2 rich plasma compared to an Ar rich plasma. This increase in the emission intensity is due to an etching of the deposited Ge since no precursor is injected in the plasma. Therefore, there is a competitive etching/deposition effect

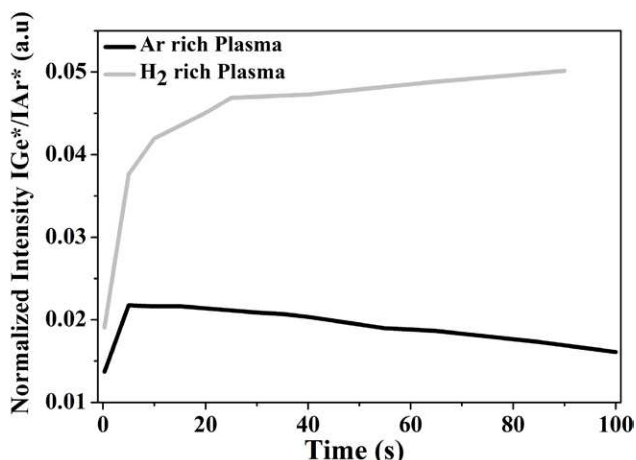

Figure 11. Normalized intensity of the OES Ge* emission line as a function of time in Ar rich [950 sccm Ar + 50 sccm H_2] and H_2 rich [50 sccm Ar + 950 sccm H_2] plasmas.

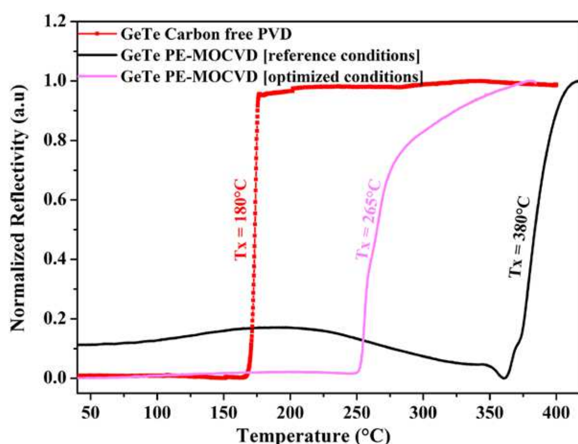

Figure 12. Evolution of the optical reflectivity as a function of temperature (10 °C/min heating ramp rate) of GeTe thin films deposited by PVD or PE-MOCVD under reference or optimized deposition plasma conditions.

during the process and it is due to the presence of hydrogen. When the hydrogen ratio increases, the Ge etching rate increases thus, deposition rate decreases.

As demonstrated above, operating parameters play a major role in the dissociation mechanisms involved in the deposition process and particularly in the control of C contamination level. It has been shown that reducing the RF power, as well as increasing the deposition pressure significantly reduces the C contamination level in Ge films. The use of a high hydrogen ratio in the H_2/Ar process gas flow also shows a reduction in C content in Ge films. Therefore, in order to optimize the quality of the GeTe layers, films are deposited under new and optimized conditions by combining parameters that have led to a low level of carbon contamination. XPS measurements on GeTe films deposited in such optimized conditions reveal a C concentration of 5 at. % which is significantly lower than the 16 at. % initially measured in the reference deposition conditions. Finally, the impact of this C level reduction on the crystallization temperature of GeTe films is investigated by reflectivity measurements. As shown in figure 12, the crystallization temperature of the GeTe films is largely reduced of more than 100 °C, from 380 °C to 265 °C by decreasing the C content in the films thanks to optimized deposition plasma conditions.

Conclusion

To summarize, homogenous and smooth layers of GeTe have been deposited by PE-MOCVD using [$Ge(NMe_2)_4$] and [$Te(i\text{-}Pr)_2$] (TDMA-Ge and DIP-Te) as Ge and Te precursors respectively. However, the GeTe films exhibit a high C contamination level. It has been shown that this contamination is mainly due to the dissociation of the Ge precursor in the deposition plasma. As a result, such high C contamination leads to a crystallization temperature for PE-MOCVD GeTe films 200 °C higher than the one generally measured for pure GeTe films obtained by PVD. It has been demonstrated that C concentration and consequently crystallization temperature are significantly reduced by properly tuning operating parameters such as RF power, pressure and H_2 rate. Indeed, it has been shown that by increasing the RF power of the plasma, the carbon level in the deposited films increases. On the contrary, carbon content significantly decreases when increasing the pressure and the H_2 rate in the plasma. In particular, hydrogen radicals are shown to play a major role in controlling C content in GeTe films. Finally, this study allowed the deposition of GeTe films with a C content as low as 5 at. % by properly tuning the deposition plasma parameters. This led to a reduction of the crystallization temperature of approximately 120 °C compared to the reference deposition conditions. These findings are of a major interest for finding routes for the deposition of phase change materials thin films, with low C concentrations, into high aspect-ratio structures from metal organic precursors for future PCRAM applications.

Acknowledgments

This work has been partially supported by the LabEx Minos ANR-10-LABX-55-01 and by the French Government program 'Investissements d'Avenir' managed by the National Research Agency (ANR) under the contract number ANR-10-IQPX-33'

References

[1] Burr G W *et al* 2010 Phase change memory technology *J. Vac. Sci. Technol.* B **28** 223

[2] Bez R and Pirovano A 2004 Non-volatile memory technologies: emerging concepts and new materials *Mater. Sci. Semicond. Process.* **7** 349–55

[3] Fantini A *et al* 2009 Comparative assessment of GST and GeTe materials for application to embedded phase-change memory devices *(IEEE) IMW Memory Workshop 2009* (Monterey, CA) pp 1–2

[4] Cho S L *et al* 2005 Highly scalable on-axis confined cell structure for high density PRAM beyond 256Mb *Symp. VLSI Technology Digest of Technical Papers* 96–97

[5] Lee J I *et al* 2007 Highly scalable phase change memory with CVD GeSbTe for sub 50 nm generation *(IEEE) VLSI Technology IEEE Symp.* (Kyoto) pp 102–3

[6] Im D H *et al* 2008 A unified 7.5 nm dash-type confined cell for high performance PRAM device *(IEEE) IEDM Electronic Devices Meeting* (San Francisco, CA) pp 1–4

[7] Betti Beneventi G *et al* 2011 Carbon-doped GeTe: a promising material for phase-change memories *Solid-State Electron.* **65–6** 197–204

[8] Fantini A *et al* 2010 N-doped GeTe as performance booster for embedded phase-change memories *(IEEE) IEDM Electronic Devices Meeting* (San Francisco, CA) pp 29.1.1–4

[9] Hubert Q *et al* 2012 Lowering the reset current and power consumption of phase-change memories with carbon-doped $Ge_2Sb_2Te_5$ *(IEEE) IMW 4th International Memory Workshop* (Milan) pp 1–4

[10] Altatech Semiconductors www.altatech-sc.com

[11] Guillon H, Bonnafous S, Decams M and Poignant F 2007 *WO Patent* 118898 A1 Europe (EP)

[12] Pelissier B *et al* 2008 XPS analysis with an ultra clean vacuum substrate carrier for oxidation and airborne molecular contamination prevention *Microelectron. Eng.* **85** 151–5

[13] Moulder J F and Chastain J 1992 *Handbook of X-Ray Photoelectron Spectroscopy: a Reference Book of Standard Spectra for Identification and Interpretation of XPS Data* (Eden Prairie: Perkin-Elmer)

[14] Gourvest E *et al* 2012 Plasma enhanced chemical vapor deposition of conformal GeTe layer for phase change memory applications *ECS J. Solid State Sci. Technol.* **1** Q119–22

[15] Gourvest E *et al* 2009 Evidence of germanium precipitation in phase-change $Ge_{1-x}Te_x$ thin films by Raman scattering *Appl. Phys. Lett.* **95** 031908

[16] Aumaille K *et al* 2000 A comparative study of oxygen/organosilicon plasmas and thin SiO_xC_yHz films deposited in a helicon reactor *Thin Solid Films* **359** 188–96

[17] Raty J-Y *et al* 2013 Vibrational properties and stabilization mechanism of the amorphous phase of doped GeTe *Phys. Rev.* B **88** 014203

[18] Zaidel A N, Prokof'ev V K and Raiskii S M 1961 *Tables of Spectral Lines* (Berlin: Veb Verlag Technik)

[19] Pearse R W B and Gaydon A G 1965 *The Identification of Molecular Spectra* (London: Chapman and Hall)

[20] Grotti M, Lagomarsino C and Frache R 2005 Multivariate study in chemical vapor generation for simultaneous determination of arsenic, antimony, bismuth, germanium, tin, selenium, tellurium and mercury by inductively coupled plasma optical emission spectrometry *J. Anal. At. Spectrom.* **20** 1365

[21] Caubet P *et al* 2008 Low-temperature low-resistivity PEALD TiN using TDMAT under hydrogen reducing ambient *J. Electrochem. Soc.* **155** H625

[22] Clay K J, Speakman S P, Amaratunga G A J and Silva S R P 1996 Characterization of a-C:H:N deposition from CH_4/N_2 rf plasmas using optical emission spectroscopy *J. Appl. Phys.* **79** 7227–33